DSP Implementation of Adaptive Notch Filters With Overflow Avoidance in Fixed-Point Arithmetic

Satoru Ishibashi, Shunsuke Koshita, Masahide Abe and Masayuki Kawamata
Tohoku University, Sendai, Japan
E-mail: satoru@mk.ecei.tohoku.ac.jp, kosita@mk.ecei.tohoku.ac.jp

***Abstract*—In this paper, we implement adaptive notch filters with constrained poles and zeros (CPZ-ANFs) using fixed-point DSP. Since the CPZ-ANFs are IIR filters that have narrow notch width, a signal can be amplified significantly in their feedback loops. Therefore, direct-form II structure suffers from high probability of overflow in its internal state. When an overflow occurs in internal state of filters, inaccurate values due to the overflow are used repeatedly to calculate the output signal of the filters. As a result, the filters do not operate correctly and therefore we have to prevent such overflow. In order to avoid the overflow, we use direct-form I structure in implementation of the CPZ-ANFs. Experimental results show that our method allows the CPZ-ANFs to operate properly on the fixed-point DSP.**

I. Introduction

Adaptive Notch Filters (ANF) is well known as a variable notch filter of which notch frequency is controlled in real time by means of an adaptive algorithm. This adaptive mechanism allows automatic detection and removal of an unknown sinusoid that is immersed in a wide-band signal such as a white noise. ANFs are widely used in many practical applications such as howling canceller [1] and wireless communication system with removal of narrowband interference [2].

To the authors' best knowledge, popular ANFs are based on second-order IIR notch filters, and two methods are well known to design the transfer functions. One is the Constrained Poles and Zeros-based ANF (CPZ-ANF) [3], and the other is the All-Pass Filter-based ANF (APF-ANF) [4], [5]. These two ANFs have been widely studied and many results such as development of adaptive algorithms [6], [7] and steady-state analyses [8]–[11] have been proposed. However, little has been reported concerning implementation of ANFs on a fixed-point Digital Signal Processor (DSP). Since ANFs have versatile practical applications as mentioned above, hardware implementation of ANFs is also an essential task. In particular, implementation of ANFs on a fixed-point DSP is quite important because fixed-point processors are superior to floating-point ones in many aspects such as circuit complexity, power consumption and processing time. For this reason, implementation of ANFs on a fixed-point DSP is the main topic of this paper.

It is important to note that ANFs are generally very difficult to implement on a fixed-point processor. To be specific, implementing ANFs without taking into account the problems on filter structures and finite wordlength effects usually result in inappropriate operation of adaptive notch filtering. Such difficulty comes from the fact that ANFs must involve narrowband IIR filters. When such narrowband filters are realized by the standard direct-form II structure and implemented on a fixed-point DSP, the feedback loop in the direct-form II structure has very large gain, causing very high probability of overflow at the internal states. Such overflow results in repeated generation of inaccurate output signals.

Motivated by this issue, this paper presents an ANF implementation method that avoids the problem of overflow on a fixed-point DSP. The proposed method focuses on the CPZ-ANF, and instead of the standard direct-form II structure we make use of the direct-form I structure to avoid the overflow. It is demonstrated by experiments on frequency estimation that the proposed method allows ANFs to properly operate on a fixed-point DSP without generating overflow.

II. Fundamentals of ANFs

A. Problem Statement of ANFs

Consider the input signal $x(n)$ of an ANF as follows:

$$x(n) = p(n) + v(n) \tag{1}$$

where $p(n)$ is the unknown sinusoid to be detected by the ANF, and $v(n)$ is a zero-mean white noise with the variance of σ_v^2. The sinusoid $p(n)$ is described by

$$p(n) = A\cos(\omega_s n + \phi) \tag{2}$$

where A and ω_s respectively denote the amplitude and the frequency of the sinusoid, and ϕ denotes the random initial phase that is uniformly distributed in $[0, 2\pi)$ and uncorrelated with $v(n)$. Also, let $y(n)$ be the output signal of the ANF.

Based on this setup, the objective of ANF is to find and remove $p(n)$ by using only the information on $x(n)$. To this end, the notch frequency of the ANF, which is denoted by ω_0, is controlled by an adaptive algorithm in such a manner that ω_0 converges to the unknown frequency ω_s of the sinusoid.

B. CPZ-ANF

As stated in Section I, this paper focuses on the CPZ-ANF [3]. Its transfer function $H_N(z)$ is given by the second-order IIR filter of the form

$$H_N(z) = \frac{1 + a(n)z^{-1} + z^{-2}}{1 + \rho a(n)z^{-1} + \rho^2 z^{-2}} \tag{3}$$

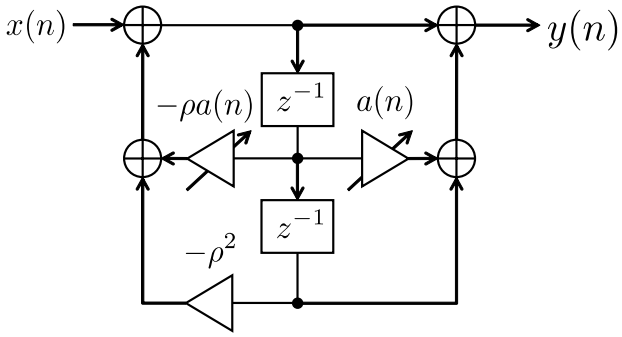

Fig. 1. Block diagram of $H_N(z)$ with direct-form II structure.

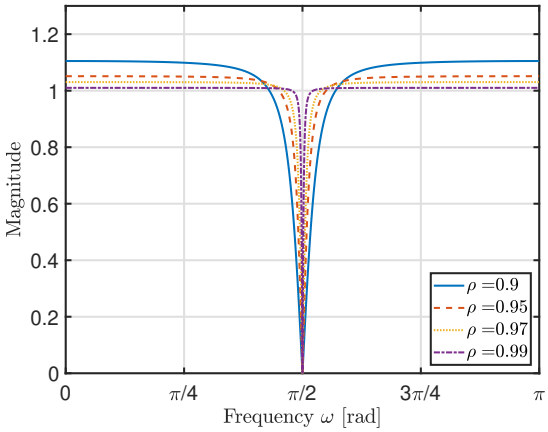

Fig. 2. Magnitude responses of $H_N(z)$ for $\omega_0 = 0.5\pi$.

where $a(n)$ is the parameter that controls the notch frequency at time n and given by

$$a(n) = -2\cos\omega_0(n) \tag{4}$$

from which it follows that $-2 \leq a(n) \leq 2$. Also, the parameter ρ in $H_N(z)$ controls the notch width, denoted by B, of the CPZ-ANF. These are related to each other by

$$B = \pi(1-\rho) \tag{5}$$

and hence ρ must satisfy $0 < \rho < 1$. Factorizing the numerator and the denominator of $H(z)$ respectively, we know that all zeros of the CPZ-ANF are on the unit circle and that all poles of the CPZ-ANF have the same angles as those of the corresponding zeros.

The block diagram of $H_N(z)$ with the direct-form II is shown in Fig. 1. Also, the magnitude responses of $H_N(z)$ for $\omega_0 = 0.5\pi$ are shown in Fig. 2.

C. Adaptive Algorithm of CPZ-ANF Based on Gradient Descent Method

Many adaptive algorithms for the CPZ-ANF have been proposed in the literature, and this paper make use of the algorithm of [12], which is based on the gradient descent

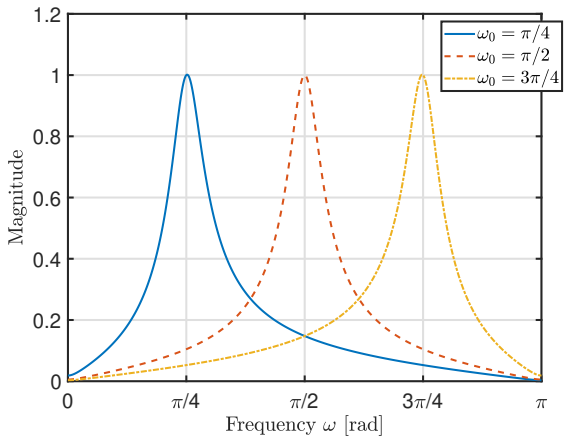

Fig. 3. Magnitude responses of gradient filter $H_S(z)$ for $\rho = 0.9$.

method. In this algorithm the cost function to be minimized is given by the mean square output of the CPZ-ANF, i.e. $E[y^2(n)]$. Therefore the notch frequency parameter $a(n)$ is controlled to minimize $E[y^2(n)]$. The update equation for $a(n)$ is given by

$$a(n+1) = a(n) - \mu\nabla(n) \tag{6}$$

where μ is the step-size parameter and $\nabla(n)$ is the instantaneous estimate of the gradient of $E[y^2(n)]$ with respect to $a(n)$. The value of $\nabla(n)$ is calculated as follows [7]:

$$\nabla(n) \triangleq \frac{\partial y^2(n)}{\partial a(n)} = 2y(n)\frac{\partial y(n)}{\partial a(n)} \tag{7}$$

$$\begin{aligned}\frac{\partial y(n)}{\partial a(n)} &\triangleq s(n) \\ &\approx x(n-1) - \rho y(n-1) - \rho a(n)s(n-1) - \rho^2 s(n-2)\end{aligned} \tag{8}$$

where the above approximation is made under the assumption that the step-size parameter is sufficiently small and the variation of $a(n)$ is sufficiently smaller than that of $x(n)$. The algorithm given in (8) means that the estimate of the gradient is obtained by the output signal $s(n)$ of the following system $H_S(z)$:

$$H_S(z) = z^{-1} - z^{-1}\rho H_N(z) \tag{9}$$

$$= \frac{(1-\rho)z^{-1} - \rho(1-\rho)z^{-3}}{1 + \rho a(n)z^{-1} + \rho^2 z^{-2}}. \tag{10}$$

Since this system is interpreted as the digital filter for calculation of the instantaneous estimate of the gradient, throughout this paper $H_S(z)$ is referred to as the gradient filter. The magnitude responses of the gradient filter for $\rho = 0.9$ is shown in Fig. 3. It is clear that the gradient filter has bandpass responses of which peak appears at the notch frequency ω_0.

In summary, the adaptive algorithm for update of $a(n)$ is given by

$$a(n+1) = a(n) - 2\mu y(n)s(n). \tag{11}$$

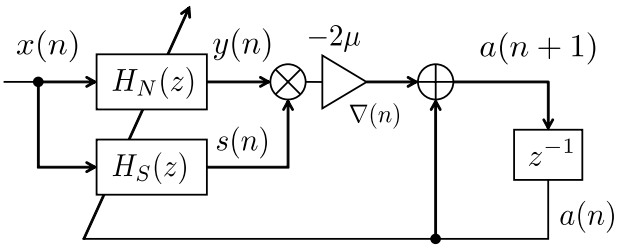

Fig. 4. Overall configuration of CPZ-ANF.

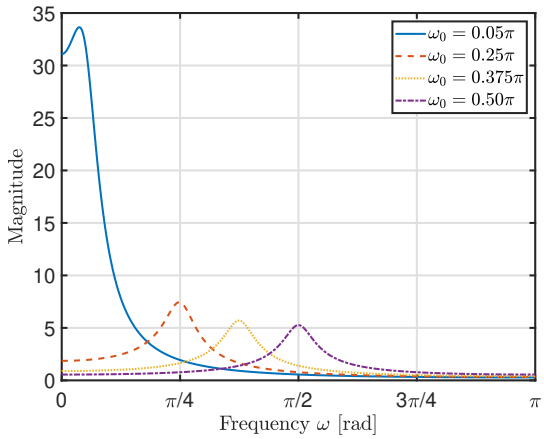

Fig. 5. Magnitude responses of $1/D_{N,S}(z)$ for $\rho = 0.9$.

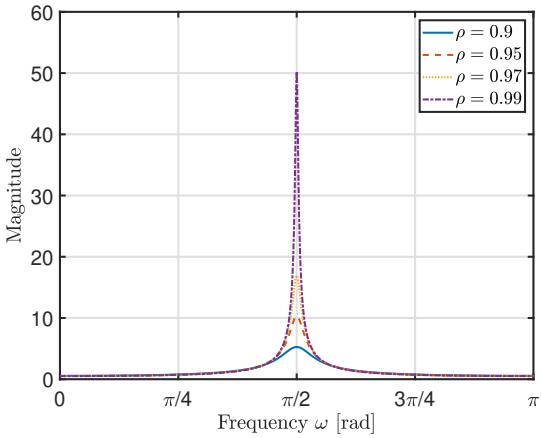

Fig. 6. Magnitude responses of $1/D_{N,S}(z)$ for $\omega_0 = \pi/2$.

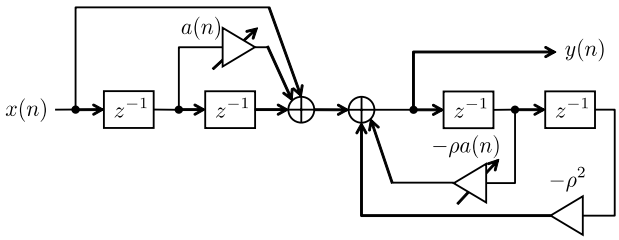

Fig. 7. Block diagram of $H_N(z)$ with direct-form I structure.

The overall configuration of the CPZ-ANF is shown in Fig. 4.

III. Proposed Method

As stated above, the CPZ-ANF is one of the narrowband IIR filters. In general, the feedback loop of such filters has very large gain because their poles tend to be very close to unit circle. Therefore standard direct-form II structure suffers from high probability of overflow because the poles precede the zeros in series. Such overflow results in repeated generation of inaccurate output signals. In order to improve this problem, we analyze the magnitude responses of the feedback loop in the CPZ-ANFs.

It is clear from (3) and (10) that $H_N(z)$ and $H_S(z)$ have the common denominator polynomial. The transfer function of the feedback loop, denoted by $1/D_{N,S}(z)$, is found to be

$$\frac{1}{D_{N,S}(z)} = \frac{1}{1+\rho a z^{-1}+\rho^2 z^{-2}} = \frac{1}{(1-\rho e^{j\omega_0} z^{-1})(1-\rho e^{-j\omega_0} z^{-1})}. \quad (12)$$

Figs. 5 and 6 show the magnitude responses of $1/D_{N,S}(z)$.

Fig. 5 shows that the peak gain becomes larger as notch frequency ω_0 gets closer to 0. Even when the notch frequency ω_0 approaches π, similar characteristics are obtained. In addition, we can see that larger ρ, i.e. narrower notch width, results in larger peak gain as shown in Fig. 6. This is due to the fact that the poles are very close to the unit circle. For these reasons, the feedback loop of $H_N(z)$ and $H_S(z)$ suffers from high probability of overflow.

To avoid such overflow at the feedback loop, we apply the following two methods: one is coefficient scaling [13], the other one is direct-form I structure.

The coefficient scaling method using L_p norm of the filter can suppress excessive amplification in the feedback loop. However CPZ-ANFs are adaptive filters of which coefficients are time-variant. Accordingly, calculation of L_p norm and division are imposed on DSP and thus the coefficient scaling method is complicated and difficult to implement on DSP. Therefore, we make use of direct-form I structure to implement CPZ-ANFs on fixed-point DSP. Fig. 7 shows the block diagram of $H_N(z)$ with direct-form I structure.

A difference between direct-form I and direct-form II structure is calculation order of feedforward block and feedback loop. While direct-form II structure first calculates the output of the feedback loop, direct-form I structure first calculates the output of the feedforward block. Overflow at the feedback loop can be avoided by implementing feedforward block first because the feedback loop causes very large gain as mentioned above. For these reasons, we apply direct-form I structure to

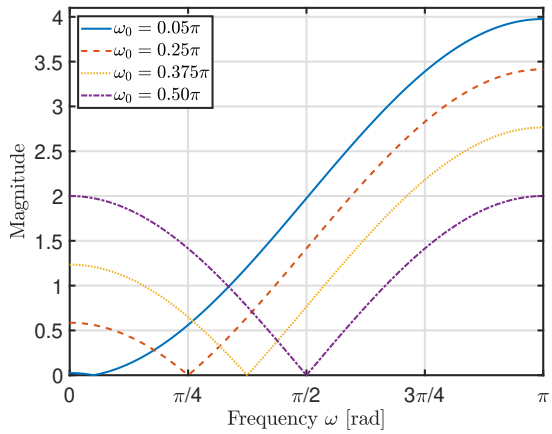

Fig. 8. Magnitude responses of $N_N(z)$.

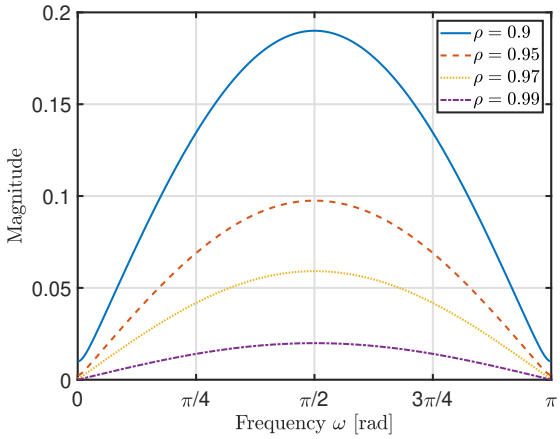

Fig. 9. Magnitude responses of $N_S(z)$.

suppress the overflow.

Even though direct-form I structure requires twice unit-delay elements compared with direct-form II structure, this does not become a serious problem because CPZ-ANFs are second-order IIR filter.

The disadvantage of direct-form I structure is that it causes larger roundoff noise since its feedforward block attenuates the input signal.

The feedforward blocks of $H_N(z)$ and $H_S(z)$ are also considered to implement CPZ-ANFs with direct-form I structure. Let $N_N(z)$ be the numerator polynomial of $H_N(z)$. Then its magnitude response is described by

$$\begin{aligned} N_N(z) &= 1 + az^{-1} + z^{-2} \\ &= 1 - 2\cos\omega_0 z^{-1} + z^{-2} \end{aligned} \tag{13}$$

$$|N_N(e^{j\omega})| = 2|\cos\omega - \cos\omega_0|. \tag{14}$$

It can be seen from (14) that the magnitude response of

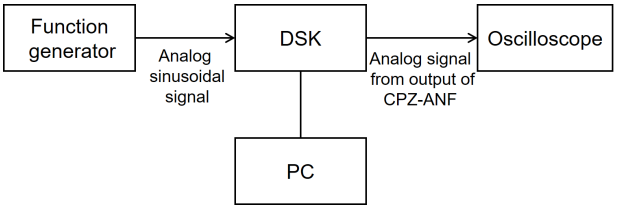

Fig. 10. Block diagram of experiments on frequency estimation.

$N_N(z)$ does not depend on ρ. Fig. 8 shows the magnitude responses of $N_N(z)$ for different notch frequencies. As shown in Fig. 8, the feedforward block of $H_N(z)$ can amplify the signal up to four times. Therefore even if direct-form I structure is used, overflow can occur at output of the feedforward block.

On the other hand, let $N_S(z)$ be numerator polynomial of $H_S(z)$. Then its magnitude response is described by

$$N_S(z) = (1-\rho)z^{-1} - \rho(1-\rho)z^{-3} \tag{15}$$

$$|N_S(e^{j\omega})| = (1-\rho)\sqrt{(1-\rho)^2\cos^2\omega + (1+\rho)^2\sin^2\omega}. \tag{16}$$

From (16), the magnitude response of $N_S(z)$ is not dependent on a. It should be noted that the feedforward block of $H_S(z)$ significantly reduces a signal and its attenuation becomes large as ρ approaches 1, as shown in Fig. 9. Hence we must pay attention to the roundoff noise in the feedforward block of $H_S(z)$.

IV. Experimental Results

Using the proposed method we implement the CPZ-ANF on a fixed-point DSP. In this section experiments on frequency estimation are presented. For simplicity, it is assumed here that the input signal consists of only a sinusoid. In other words, the noise term $v(n)$ is assumed to be zero.

A. Specification of Fixed-Point DSP

In the experiments we use the TMS320C5x DSP Starter Kit (DSK) produced by Texas Instruments Inc., and this DSK is equipped with the TMS320C50DSP. This is the 16-bit fixed-point DSP that can be programmed by assembly language to carry out real-time signal processing. The DSK used here has a 20-MHz system clock and the TMS320C50DSP provides a product-sum instruction that can be processed in a single cycle. Also, the TMS320C50DSP includes a 32-bit accumulator and hence 16-bit $\times$ 16-bit multiplications can be processed. Also, the DSK can deal with input signals with voltage of up to 3.3 V [14].

B. Configuration of Experiments

The system for the experiments on frequency estimation is shown in Fig. 10. The function generator used here is the Agilent 33120A produced by Keysight Technologies. This function generator provides an analog sinusoidal signal, which is sampled and quantized in the DSK and becomes the input signal $x(n)$ of the CPZ-ANF that is programmed in the

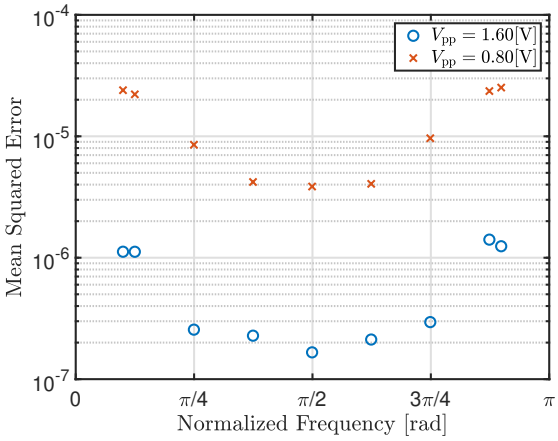

Fig. 11. MSE on frequency estimation.

TMS320C50DSP. The output signal of the DSK is the D/A-converted-signal that is given from $y(n)$, i.e. the output signal of the CPZ-ANF. This signal is measured by the oscilloscope and used in order to judge whether the adaptive algorithm of the CPZ-ANF attains the steady state. The PC, which is connected to the DSK, acquires the data sequences of $\{a(n)\}$ of the CPZ-ANF at the steady state. The sequences $\{a(n)\}$ are then converted to the data sequences of the steady-state notch frequencies by means of the following relationship:

$$\omega_0(n) = \cos^{-1}\left(-\frac{a(n)}{2}\right). \tag{17}$$

Note that this relationship can be easily derived from (4). The values of μ and ρ in the CPZ-ANF are fixed, and the initial value of the notch frequency parameter is set to be $a(0) = 0$.

In the experiments, the sampling frequency of the DSK is set to be 8,013 Hz. Also, the TMS320C50DSP is configured in such a manner that the fixed-point data to be processed has 3 integer bits and 13 fractional bits. This means that the TMS320C50DSP can deal with signals with the values of $[-4, 4)$. This configuration is due to the aforementioned fact that the feedforward block of $H_N(z)$ has the maximum peak gain of 4. According to this configuration, in order to avoid the overflow in the CPZ-ANF the amplitude of $x(n)$ is restricted to the range of $[-1, 1)$, which corresponds to analog inputs within the voltage from -0.82 to 0.82 V.

C. Results

The experimental results on the frequency estimation are shown in Tables I and II, which respectively correspond to the cases of 1.6 V peak-to-peak and 0.8 V peak-to-peak for the analog sinusoidal signals. The results shown in Tables I and II consist of the estimated frequency, the estimation error, the error variance, and the Mean Square Error (MSE) in terms of normalized frequency. The MSE is also shown in Fig. 11.

Table I tells us that estimated frequency is very close to the frequency of the sinusoid and shows that the CPZ-ANF implemented by the proposed method properly operates on the fixed-point DSP. Also, it should be noted here that the error variance and the MSE become smaller as the frequency of the sinusoid goes closer to $\pi/2$ rad. This result is due to the feedforward block of $H_N(z)$ has the peak gain at $\omega = \pi/2$, which minimizes the effect of roundoff noise.

The result of Table II also shows that the frequency estimation is successfully performed by the CPZ-ANF implemented by the proposed method. However, it is also found from Fig. 11 that the MSE in the case of 0.8 V peak-to-peak input becomes larger than the case of 1.6 V peak-to-peak input. This performance degradation comes from the small gain of the feedforward block of $H_S(z)$, causing large roundoff noise. Another reason of this degradation is the smaller amplitude of the analog input, which results in worse SNR than the case of 1.6 V peak-to-peak input.

In addition, it is also found from Tables I and II the estimation error shows negative value in all cases. This result comes from the fact that small noise is included in the analog input and this noise leads to the biased estimation. As is well known, the CPZ-ANF gives biased estimation when the input signal includes noise [9].

V. Conclusion

This paper has proposed a method for implementation of the CPZ-ANF on a fixed-point DSP. Our method makes use of the direct-form I structure in order to reduce the possibility of overflow in the CPZ-ANF on the fixed-point DSP. Experimental results have demonstrated that the CPZ-ANF implemented by the proposed method successfully estimates the frequency of the input sinusoid.

Future works include improvement of estimation accuracy of the CPZ-ANF and implementation of other ANFs on a fixed-point DSP.

References

[1] K. Mashita and N. Aikawa, "Howling canceller with speech suppression filter," *IEICE Trans. Fundamentals (Japanese Edition)*, vol. J99-A, no. 8, pp. 332–335, Aug. 2016, in Japanese.

[2] A. Mvuma, S. Nishimura, and T. Hinamoto, "BER analysis for a QPSK DS-CDMA system over rayleigh channel with a NBI suppression complex adaptive IIR notch filter," *IEICE Trans. Fundamentals*, vol. E94-A, no. 11, pp. 2369–2375, Nov. 2011.

[3] A. Nehorai, "A minimal parameter adaptive notch filter with constrained poles and zeros," *IEEE Trans. Acoust., Speech, Signal Process.*, vol. 33, no. 4, pp. 983–996, Aug. 1985.

[4] J. A. Chambers and A. G. Constantinides, "Frequency tracking using constrained adaptive notch filters synthesised from allpass sections," *IEE Proc. F - Radar and Signal Process.*, vol. 137, no. 6, pp. 475–481, Dec. 1990.

[5] P. A. Regalia, *Adaptive IIR Filtering in Signal Processing and Control*. Marcel Dekker, 1994.

[6] S. Nakamura, S. Koshita, M. Abe, and M. Kawamata, "A new adaptive notch filtering algorithm based on normalized lattice structure with improved mean update term," *IEICE Trans. Fundamentals*, vol. E98-A, no. 7, pp. 1482–1493, July 2015.

[7] S. Kinjo and N. Kambayashi, "An IIR adaptive notch filter utilizing a modified stochastic gradient algorithm," *IEICE Trans. Fundamentals (Japanese Edition)*, vol. J74-A, no. 7, pp. 1014–1022, July 1991, in Japanese.

TABLE I
RESULT OF FREQUENCY ESTIMATION BY DSK. (1.6 V PEAK-TO-PEAK FOR ANALOG INPUT)

Frequency of sinusoid f [Hz]	Estimated frequency f_0 [Hz]	Error [Hz]	Error variance	MSE
400	398.733	-1.267	2.184×10^{-1}	1.121×10^{-6}
500	498.722	-1.278	1.872×10^{-1}	1.120×10^{-6}
1000	999.370	-0.630	1.958×10^{-2}	2.557×10^{-7}
1500	1499.393	-0.607	2.845×10^{-3}	2.281×10^{-7}
2000	1999.483	-0.517	2.666×10^{-3}	1.662×10^{-7}
2500	2499.417	-0.583	4.317×10^{-3}	2.120×10^{-7}
3000	2999.313	-0.687	7.688×10^{-3}	2.950×10^{-7}
3500	3498.527	-1.473	1.225×10^{-1}	1.409×10^{-6}
3600	3598.606	-1.394	7.905×10^{-2}	1.243×10^{-6}

TABLE II
RESULT OF FREQUENCY ESTIMATION BY DSK. (0.8 V PEAK-TO-PEAK FOR ANALOG INPUT)

Frequency of sinusoid f [Hz]	Estimated frequency f_0 [Hz]	Error [Hz]	Error variance	MSE
400	393.769	-6.231	1.549×10^{-1}	2.397×10^{-5}
500	494.024	-5.976	3.309×10^{-1}	2.216×10^{-5}
1000	996.301	-3.699	1.742×10^{-1}	8.520×10^{-6}
1500	1497.385	-2.615	2.564×10^{-3}	4.205×10^{-6}
2000	1997.498	-2.502	1.266×10^{-2}	3.858×10^{-6}
2500	2497.432	-2.568	6.291×10^{-3}	4.059×10^{-6}
3000	2996.051	-3.949	8.557×10^{-2}	9.641×10^{-6}
3500	3493.812	-6.188	4.592×10^{-2}	2.358×10^{-5}
3600	3593.610	-6.390	1.293×10^{-1}	2.519×10^{-5}

[8] S. Koshita, Y. Noguchi, M. Abe, and M. Kawamata, "Analysis of frequency estimation MSE for all-pass-based adaptive IIR notch filters with normalized lattice structure," *Signal Process.*, vol. 132, pp. 85 – 95, Mar. 2017.

[9] Y. Xiao, Y. Takeshita, and K. Shida, "Steady-state analysis of a plain gradient algorithm for a second-order adaptive IIR notch filter with constrained poles and zeros," *IEEE Trans. Circuits Syst. II*, vol. 48, no. 7, pp. 733–740, July 2001.

[10] A. Mvuma, S. Nishimura, and T. Hinamoto, "State-space approach to steady-state analysis of adaptive IIR notch filters," in *Proc. IEEE Midwest Symp. Circiuts Syst.*, Aug. 2005, pp. 883–886.

[11] Y. Xiao, Y. Takeshita, and K. Shida, "Tracking properties of a gradient-based second-order adaptive IIR notch filter with constrained poles and zeros," *IEEE Trans. Signal Process.*, vol. 50, no. 4, pp. 878–888, Apr. 2002.

[12] J. F. Chicharo and T. S. Ng, "Gradient-based adaptive IIR notch filtering for frequency estimation," *IEEE Trans. Acoust., Speech, Signal Process.*, vol. 38, no. 5, pp. 769–777, May 1990.

[13] L. Jackson, *Digital Filters and Signal Processing*. Kluwer Academic Publishers, 1996.

[14] Texas Instruments Inc., *TMS320C5x Digital Signal Processor User's Manual*. Texas Instruments Japan Ltd., 1994, in Japanese.